A Europium(III) Complex with an Unusual Anion-Cation Interaction: A Luminescent Molecular Thermometer for Ratiometric Temperature Sensing

Mani Outis[a], Prof. César A. T. Laia[a], Dr. M. Conceição Oliveira[b], Dr. Bernardo Monteiro[*b,c], Dr. Cláudia C. L. Pereira [*a]

[a] LAQV-REQUIMTE, Departamento de Química, Universidade Nova de Lisboa, 2829-516 Caparica, Portugal.

[b] Centro de Ciências e Tecnologias Nucleares (C^2TN), DECN, Instituto Superior Técnico, Estrada Nacional 10, 2695-066 Bobadela, Portugal.

[c] Centro de Química Estrutural (CQE), DECN, Instituto Superior Técnico, Estrada Nacional 10, 2695-066 Bobadela, Portugal.

Abstract

An unusual anion-cation interaction, thermally sensitive, characteristic of the anion $[Eu(FOD)_4]^-$ and presented by complex $[CHOL][Eu(FOD)_4]$ (**1**), (CHOL is choline), that affect both quantum yield and thermochromic behavior, prompted the design of a new Eu^{3+}-based ratiometric thermometer up to temperatures of 95 °C. This new luminescent ratiometric thermometer uses a thermally excited state absorption of the Eu^{3+} ion. This reusable temperature-sensitive luminescent complex was synthesized for the first time and presented a range of relative sensitivity between 0.45% C^{-1} at 25 ºC, with increase to 7.0 % C^{-1} at 95 ºC. Two thermochromic parameters I_{613}/I_{616} and I_{616}/I_{613} are temperature dependent and present a ratiometric relation with temperature.

Confinement of compound **1** in a transparent film of polysulfone (**1-PSU**) induced higher thermal stability of **1** while its luminescence presented a strong temperature dependence of the emission intensity.

1. Introduction

Non-invasive methods for sensing and mapping temperature, able to work at the nanoscale, have emerged as a recent new field of research as an alternative to conventional methods that present some fragilities under certain analytical conditions.

The use of lanthanide compounds as thermal probes was recently and exhaustively reviewed by Carlos and co-workers.[1,2] Among these sensors, Eu^{3+}-based luminescent complexes have been widely investigated to be used as molecular thermometers over conventional thermometers.[3-8] The Eu^{3+} luminescence is affected by temperature and can be monitored by the induced changes in the integrated emission intensity of a single transition, a pair of transitions, spectral shifts, the band shape or bandwidth of a certain transition and lifetime. This topic has been widely explored since 2010, mainly due to the enormous importance of luminescence thermometry in nanotechnology and nanomedicine.[9-12] $Eu(tta)_3$ complex (tta = 3-thenoyltrifluoroacetonate) was presented as the first example with real-time thermogenesis in a single HeLa cell, with temperature variations as low as 1 °C, when dissolved in DMSO. [13]

In Eu^{3+} doped systems, the ratio of the emission intensity between $^5D_1 \rightarrow {}^7F_J$ and one of the emission bands from $^5D_0 \rightarrow {}^7F_1$ or $^5D_0 \rightarrow {}^7F_2$ has been used as a possible coupling scheme for temperature sensing.[14-19] For example, the heterotetranuclear $[Eu_2Na_2(nta)_2(CF_3CO_2)_4(naphCO_2)_2(tpm^*)_2]\cdot H_2O$ (1) [nta^- = 1-(2-naphthoyl)-3,3,3-trifluoroacetonate; $naphCO_2^-$= naphthalene-2-carboxylate; tpm* = tris(3,5-dimethyl-1-pyrazolyl)methane] has a strong temperature dependency of the total emission intensity and lifetime between 0 and 60 °C, extrapolated from the integrated intensity ratio between the $^5D_0 \rightarrow {}^7F_2$ and $^5D_0 \rightarrow {}^7F_1$ transitions.[3]

A dinuclear Eu^{3+} complex with a structure of [BP-$(Eu)_2$-$(ODA)_3$] (BP = 2,20-bipyridine-6,60-dicarboxylic acid bis(N-hydroxysuccinimide) ester, ODA = diglycolic acid) presents a totally reversible emission spectra at the highly narrow $^5D_0 \rightarrow {}^7F_2$ transition band in response to temperature variation between 10 °C to 60 °C.[20] This methodology takes into consideration that Eu^{3+} complexes have different number of coordinated water molecules to the emissive Eu^{3+} centre, since a significant increase of emission intensity at 616 nm (shoulder), relative to the emission at 613 nm, was observed.

In this context, this work presents the temperature dependence of the photophysical spectral properties of a tetrakis-1,1,1,2,2,3,3-heptafluoro-7,7-dimethyloctane-4,6-dionate-Eu^{3+} anionic complex with thermochromism in the visible range. An unusual thermochromic behaviour, similar to the previously observed for $[P_{6,6,6,14}][Eu(FOD)_4]$,[21] $[P_{6,6,6,14}]^+$ is trihexyltetradecylphosphonium cations, was also identified in the $[CHOL][Eu(FOD)_4]$ complex (**1**), foreseeing the design of new luminescent temperature probes. An equilibrium reflecting a temperature-dependent degree of asymmetry on the coordination of the Eu^{3+} ion leads to a dramatic change in the intensity of the hypersensitive transition $^5D_0 \rightarrow {}^7F_2$, which reflects the temperature to which the complex is exposed. Here, we present linear and polynomial ratiometric relations of emission band intensity with temperature, seldom observed in mononuclear complexes.[22,23] The type of thermometry described here, can be classified as lanthanide-based intensity molecular thermometer,[20,24] where the intensity and shape of the luminescence lines of Eu^{3+} ion depend on several parameters including temperature as one of the most susceptible.

2. Results and Discussion

2.1 Temperature dependence of the photophysical properties of 1

The excitation spectra of **1** (experimental section) was monitored within the Eu^{3+} $^5D_0 \rightarrow {}^7F_2$ transition maxima and is completely dominated by a broad band ranging in the UV (ca. 320-400 nm) with maximum of 344 nm at 25°C, with a regular increment until 354 nm at 110 °C. This band is attributed to ligand-cantered ($S_1 \rightarrow S_0$) transitions of the FOD-diketonate ligand and is partially overlapped by a moderate intense peak at 393 nm attributed to $^7F_0 \rightarrow {}^5L_6$ transition of the Eu^{3+} ion.[25] Figure 1 shows the excitation spectra of **1** from 25 °C to 110 °C recorded every 5 °C during sample heating.

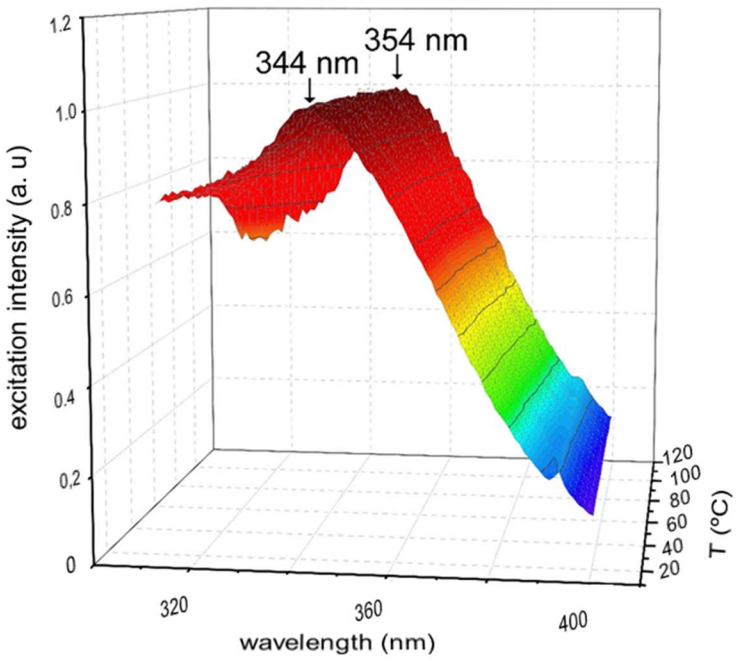

Fig. 1. Normalized intensity (relative to the most intense peak at 25 °C) of the excitation spectra of **1** acquired from 25 °C (first line) to 110 °C (last line) and monitoring the emission at their corresponding maximum, 613 nm (vertical axis: excitation, a.u.; horizontal axis: wavelength, nm; out of plane axis: Temperature, ºC).

The red shift of the maximum intensity can be explained by the structural modification of the coordinated β-diketonate ligand induced by temperature increase.[21] For the $[P_{6,6,6,14}][Eu(FOD)_4]$ ionic liquid, it was observed a gradual colour change from the familiar light yellow to a deep red at temperatures close to 80 °C, attributed to partial β-diketonate decomplexation, with concomitant establishment of a strong anion-cation interaction.[21] Additionally, it was also reported that the cations of [Eu(β-diketonate)$_4$] salts can have a strong influence on the structure of the anion and consequently on the optical properties of the complexes.[26] For complex **1**, the temperature perturbation affected the coordinating ligand, lowering its excitation energy, thus shifting the excitation spectra closer to the visible region in 10 nm. This effect was previously achieved through the modification of a β-diketonate ligand to a suitable expanded π-conjugated system, lowering the energy gap between the lowest singlet excited state (S_1) and the lowest triplet state (T_1).[27]

The emission spectra of complex **1** exhibits the typical series of narrow lines attributed to the $^5D_0 \rightarrow {}^7F_{0-4}$ transitions of the Eu^{3+} ion (Figure 2a). When we plot the emission spectra of **1** with increasing temperature, one can see the appearance of a shoulder at 616 nm which increases in intensity with temperature, reflecting the increase in the degree of asymmetry around the Eu^{3+} centre (Fig. 2a and 2b).[28]

Taking advantage of this unique characteristic, we propose a methodology to evaluate the thermal sensitivity of Eu-based salts as molecular thermometers by using a ratiometric response between the most intense signal of the transition band $^5D_0 \rightarrow {}^7F_2$ and the intensity of the shoulder at 616 nm.

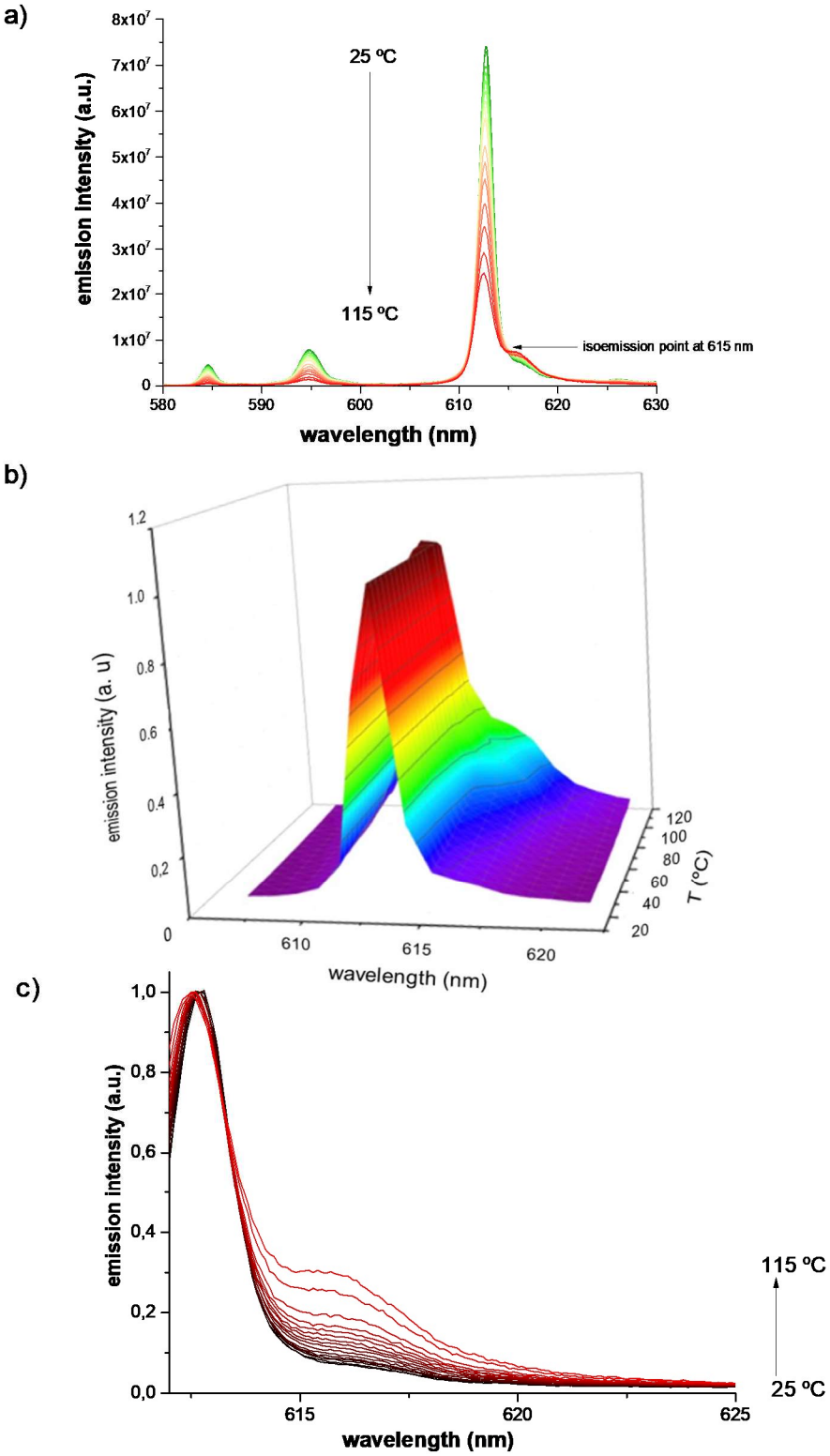

ig. 2. a) Normalized emission spectra of **1** relative to the most intense $^5D_0 \rightarrow {}^7F_2$ transition band (25 °C), from 25 (blue line) to 110 °C (red line) with a 5°C step size between each measurement. $\lambda_{exc.}$ between 344 and 354 nm according with temperature. * 616 nm shoulder. b) 3D representation of $^5D_0 \rightarrow {}^7F_2$ transition

band profile evolution with temperature (vertical axis: excitation, a.u.; horizontal axis: wavelength, nm; out of plane axis: Temperature, ºC). c) Enlargement of 616 nm shoulder emission zone normalized to the respective $^5D_0 \rightarrow {}^7F_2$ transition band.

A large $^5D_0 \rightarrow {}^7F_1$ magnetic transition band splitting of 10 nm was observed which indicates a low site symmetry for the Eu^{3+} center. The integrated emission intensity ratio between $^5D_0 \rightarrow {}^7F_1$ (magnetic dipole transition) and $^5D_0 \rightarrow {}^7F_2$ (electric dipole transition), referred as AS (Asymmetric Ratio), systematically increases from 4.7 to 9.0 as the temperature increases from 25 to 110 °C. This suggests a significant and gradual distortion in the ligand field as consequence of partial ligand de-coordination during temperature increase. Alternatively, we present here a ratiometric method involving the ratio between the intensities of two extremely narrow bands, very close in energy; the shoulder at 616 nm and the maximum intensity of the $^5D_0 \rightarrow {}^7F_2$ transition at 613 nm. The emission intensity at 613 nm decreases with an increase of temperature from 25 °C to 110 °C, conversely the emission intensity at 616 nm increases with the increase of temperature. From the spectral profile change, we observe a clear iso-emission point at 615 nm (Fig. 2 c).

Hereupon, such unique emission and coordination properties of Eu^{3+} ion make it an extremely important probe, capable of a ratiometric relation in extremely narrow emission bands close in energy. Similar spectroscopic considerations, although with a different experimental approach, were previously reported by Yuasa and Kawai for the water soluble dinuclear europium (III) complex [$Eu_2BP(ODA)_3$] (BP = 2,20-bipyridine-6,60-dicarboxylic acid bis(N-hydroxysuccinimide)ester, ODA = diglycolic acid).[20]

A fluorescence lifetime (ϖ) of 1.26 ms was determined for **1,** at room temperature, with monoexponential fluorescence decays curves, with the emission monitored at 612 nm and the excitation at 344 nm (Fig.S2, ESI for details). After heating **1** at 110 ºC, until complete colour change of the solid to purple, the fluorescence lifetime was measured at room temperature with the emission monitored at 612 nm and the excitation at 354 nm (Fig. S3, ESI for details). A significant decrease in lifetime was observed (ϖ=0.98 ms) which is a clear indication of a different emitting specie. Also, exposing **1** to heat, until colour change, it

was observed a drastic decreased of luminescence quantum yield, ϕ, in the solid state, from 82 to 44%, respectively without heating and after prior heating before experiment performed at room temperature. Fig. 3 evidences the thermochromic behaviour of **1** at 25 ºC and 100 °C, under daylight and under UV 366 nm light.

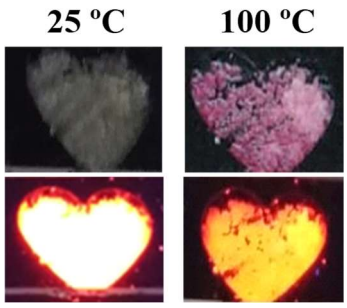

Fig. 3. Colour evolution of **1** upon heating from 25 to 100 °C. Under daylight (up) and UV light (bottom) for each temperature.

Attempts to obtain good quality crystals of **1** were fruitless, mainly due to an increase in disorder within the crystalline lattices induced by fluorine from the diketonate aliphatic chain. The structural modification due to sample heating was alternatively explored using FT-IR spectroscopy (Fig. S4 and S5, ESI). Particularly, the absorption band at 1590 cm^{-1}, that can be attributed to the stretching mode of -C-O from β-diketonate ligands complexed with Eu^{3+}, which moved towards lower wavenumbers 1577 cm^{-1} with band broadening when heated (Fig. S4, ESI).[29] This can be ascribed to the formation of an hydrogen bond between FOD and CHOL moieties, as O···H–O, that weakens the C–O bond of the β-diketonate ligand. In addition, the band at 1632 cm^{-1} ascribed to the bending vibration of O-H (δ_{as}) decreases slightly to 1629 cm^{-1}, presumably also due to weakening of O-H bond of choline. The broad band around 3400 cm^{-1}, that can be seen at 20 °C and disappears after heating for 20 min. at 100 °C, is the bending vibrations of H-O-H from water adsorbed in the sample. The medium intensity bands between 2860-2970 cm^{-1} are attributed to the typical symmetric and asymmetric C−H stretching vibrational modes of the CH_3 groups. The alkene

C-C bond is responsible for the band at 1514 cm^{-1}, and the bands between 600-1200 cm^{-1} and 800-900 cm^{-1} are assigned to the stretching modes of the C–C and C–F respectively.

Taking into consideration the melting point of complex **1** (starting at around 105 °C), temperature at which the luminescence drastically decreases due to a less "rigid" environment of the Eu^{3+} centre, the maximum temperature studied was relatively low due to instrumental limitations. The selection of an alternative cation, capable of establishing the here discussed anion-cation interactions, will certainly allow reaching upper limits for the melting temperature.

2.2 Ratiometric temperature sensing

The experiments of calibration were run in duplicate, in consecutive days, with the same batch of **1**. Upon temperature increase different ratiometric relations of band intensity emissions were found; I_{613}/I_{616}, I_{616}/I_{613} and $I_{5D0\rightarrow7F1}/I_{5D0\rightarrow7F2}$.

a) I_{613}/I_{616}

We present here a ratiometric method involving the ratio between the intensities of two extremely narrow bands, very close in energy; the shoulder at 616 nm and the maximum intensity of the $^5D_0\rightarrow{}^7F_2$ transition at 613 nm (Fig. 2a). The emission intensity at 613 nm decreases with an increase of temperature from 25 °C to 100 °C, conversely the emission intensity at 616 nm increases with the increase of temperature.

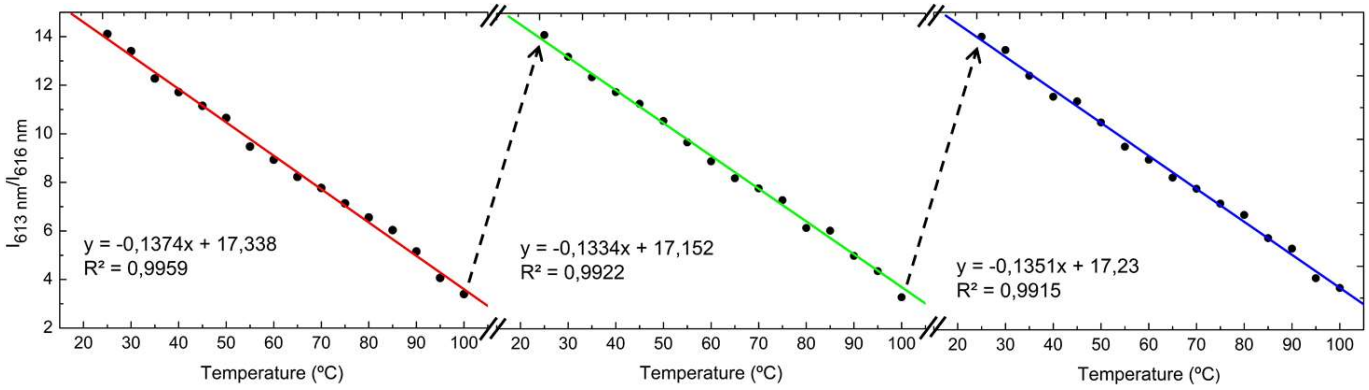

Fig. 4. Calibration plots from 25 °C to 100 °C with I_{613}/I_{616} ratio vs Temperature for three repeated cycles.

As can be inferred from the data of Figure 4, the reproducibility and reversibility of the calibration curve is very good due to the high thermal stability of **1** during at least three heating/cooling cycles. This was additionally confirmed by preforming three consecutive cycles of differential scanning analysis (DSC) (Fig. S5, ESI). Beyond this temperature, others phenomenon, like melting, start to interfere with the ratiometric relations presented here.

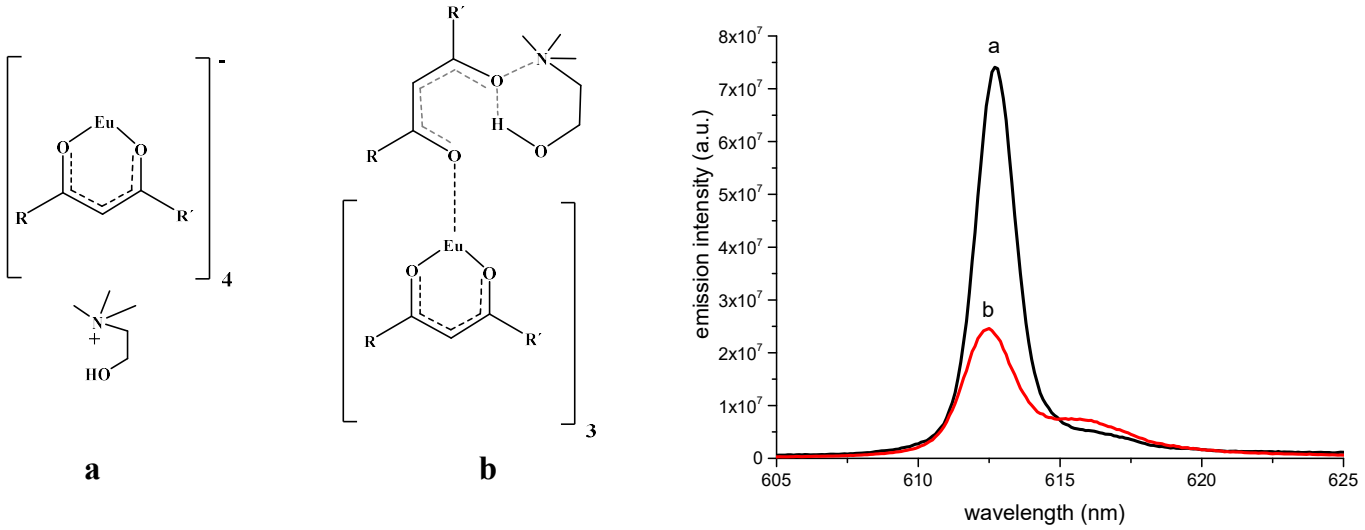

Fig. 5. Suggested structures for the minimum (**a**) and maximum (**b**) anion/cation interaction achieved respectively at 25 ºC and 100 ºC. On the right, emission spectra of **a** at 25 ºC (black line) and **b** at 100 ºC (red line) respectively.

The linear fit found evidences an absolute sensitivity (S_a, $S_a=\delta I/\delta T$, % C^{-1}) of 27% C^{-1} a value that depends only on the degree of the thermally induced variations in the selected temperature range. [30]

Linearity is one of the desired features in thermal sensing since it guarantees a constant thermal sensitivity in the entire working temperature of the thermal probe. Systems that show significant changes in

luminescence properties, attributable to discrete temperature changes, will provide larger thermal sensitivities.

Relative sensitivity is one of the most important parameters that ensure the accuracy of temperature sensing. It is used, together with temperature uncertainty, to characterize the thermometer performance. [31,32]

The relative sensitivity is defined as follows:

$$Sr = \frac{(\frac{\delta I}{\delta T})}{I}$$

Where I is the ratio I_{613}/I_{616} emission intensity for the correspondent T.

The results show that this new ratiometric thermometer can be used in a wide temperature range, and it is especially sensitive in the range 80 ºC−100 ºC, having a high relative sensitivity up to 7% C^{-1} at 95 ºC (Fig. 6).

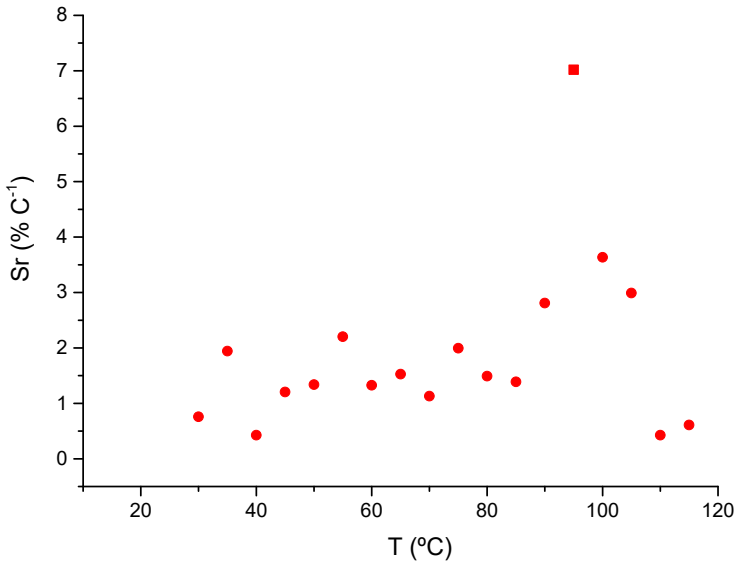

Fig. 6. Relative sensitivity, Sr (% C^{-1}) of **1**.

Other types of ratiometric optical nanothermometers, with linear response to temperature, are reported in Tab. 1.

Tab. 1. Comparison of sensitivity of other recently reported ratiometric nanothermometers with **1**. Materials, the temperature range of analysis (ΔT), and maximum relative sensitivity (S_m% C^{-1}) under the temperature range.

Material	ΔT(ºC)	S_m (% C^{-1})	Ref.
% Tm, 3% Yb -doped glass	21.8-451.8	0.35	[33]
ZrO_2:Eu^{3+} nanocrystals	6.8-206.8	1.8	[34]
Tb/Eu-BTC MOF films	25-110	16.1	[35]
Yb^{3+}, Nd^{3+}@$NaYF_4$	26.8-139.8	9.6	[36]
phen-polymer@Eu,Tb_tfac	13.1-186.8	2.3	[37]
CHOL[Eu[FOD)$_4$]	25.0-100.0	7.0	This work

Tab. 1 summarizes some of the latest achievements of high-resolution thermal sensing from the analysis of lanthanides luminescence. It shows that many luminescent systems can be used as simple light-emitting materials for nanothermometry.

b) I_{616}/I_{613}

A different ratiometric relation was also found and can be defined by the polynomial equation; I_{616}/I_{613}= $4x10^{-5}T^2$-0.002T+0.118 with r^2 = 0.9948 (Fig. 7 a). Thus, the changes in site symmetry, can be also related polynomially, with the temperature to which complex **1** is exposed. Globally, the polynomial fit found for **1** evidence an increase in sensitivity (S_m is maximum sensitivity) at higher temperatures, reaching a maximum value of 0.75% C^{-1} at 110 °C. Additionally, and as a complement, an almost linear relation was found for log(I_{616}/I_{613}) versus temperature above 45 °C (Fig. 7 b).

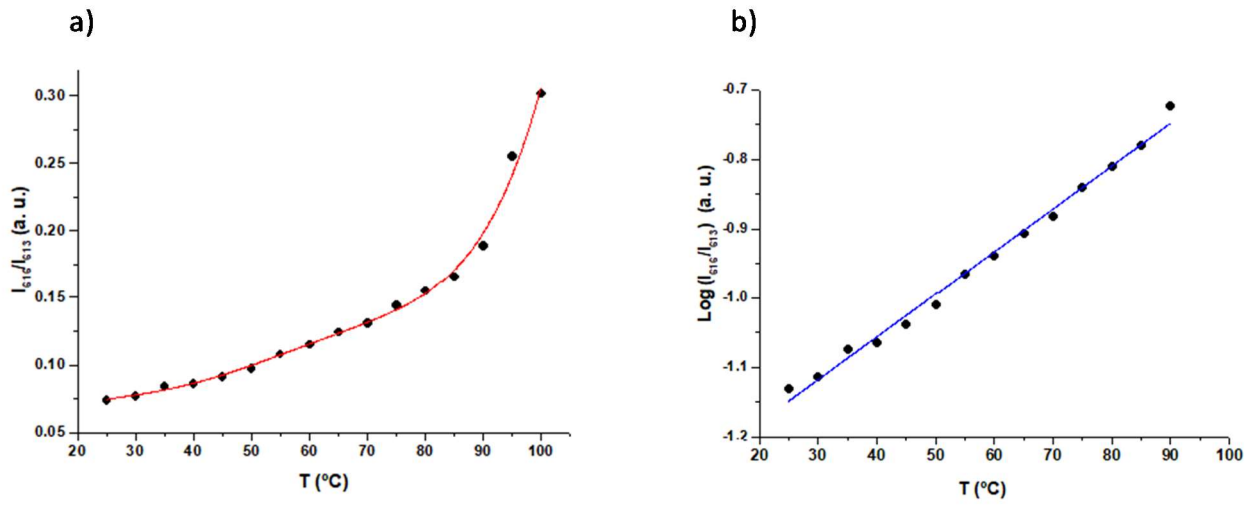

Fig. 7. a) Temperature dependent I_{616}/I_{613} ratio of **1** from 25 to 110 °C with polynomial fit $I_{616}/I_{613}= 5x10^{-4}T^2-0.01236T-0.033$ with $r^2 = 0.991$. b) $Log(I_{616}/I_{613})$ versus temperature above 45 ºC with linear fit $logI_{616}/I_{613}= 6.2x10^{-3}T-1.30$, $r^2= 0.9916$

c) $I_{5D0\rightarrow7F1}/ I_{5D0\rightarrow7F2}$

The ratio between normalized intensity of $^5D_0\rightarrow{}^7F_1$ (magnetic dipole transition) and $^5D_0\rightarrow{}^7F_2$ (electric dipole transition) decreases with temperature increase, which means that emission profile of **1** changes during sample heating, accompanied by a substantial decrease of complex symmetry around Eu^{3+} centre.[28]

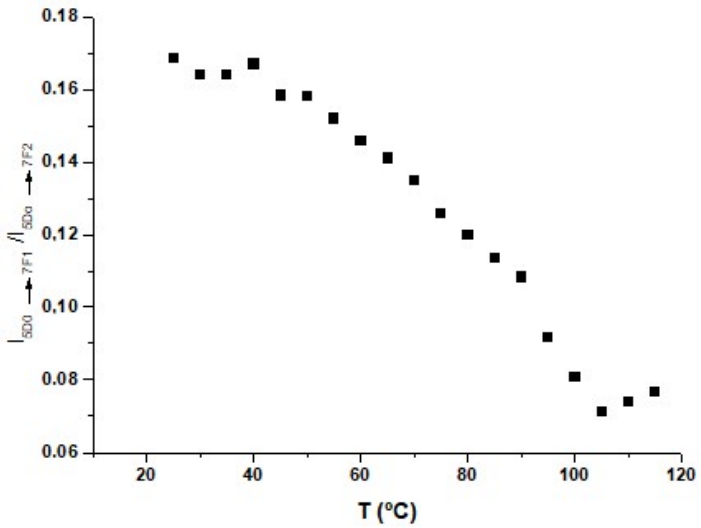

Fig. 8. Complex **1** $I_{5D0\rightarrow7F1}/I_{5D0\rightarrow7F2}$ maximum emission intensity as a function of temperature.

2.3 Non-ratiometric temperature sensing

The photoluminescence of **1**, as a function of temperature, was also explored in terms of the $^5D_0 \rightarrow {}^7F_2$ integrated total intensity, although this methodology cannot be considered a ratiometric method for temperature sensing, it is extensively reported in temperature sensing studies regarding Eu^{3+} compounds.[3,38,39] In the 25 ºC-115 °C range, the emission decreases with an average of 0.94 %°C^{-1} reaching its minimum at 115 °C where it reaches 20% of the 25 °C intensity, as shown in Fig. 9.

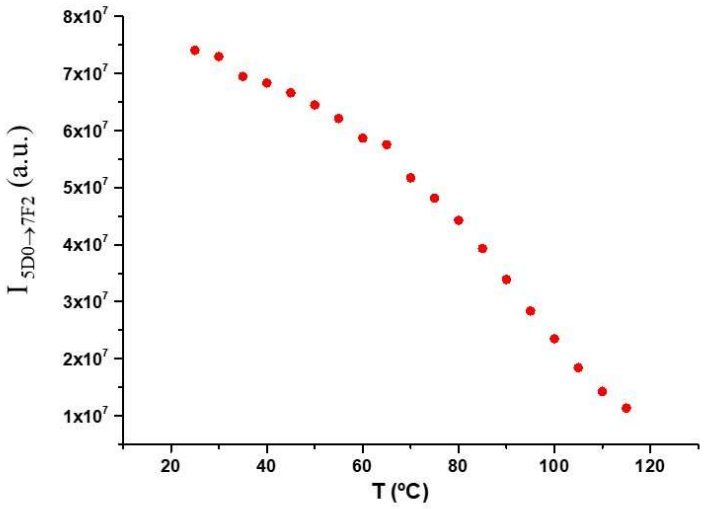

Fig. 9. Complex **1** $^5D_0 \rightarrow {}^7F_2$ maximum total emission intensity as a function of temperature

2.4 Confinement of [CHOL][Eu(FOD)$_4$] in polysulfone film

Confinement of complex **1** within a polysulfone membrane, **1-PSU**, reduces the complex mobility which hinders the anion-cation interaction during heating. For the **1-PSU** film, the reduction in the emission intensity of Eu^{3+} is not accompanied by any significant changes in the respective profile (Figure 9).[40] In this case, the usually observed and commonly reported temperature-dependent luminescence intensity was observed, with a linear fit from 60 to 120 °C and a quantum yield, ϕ, at room temperature, of 54 %. This functionalized polymer, containing lanthanide complexes, will effectively improve mechanical strength and

thermal stability of pure Eu^{3+} complexes. Thermogravimetric analysis (Fig. S6, ESI) detected a weight loss attributed to complex **1** decomposition starting at temperatures close to 230 °C, about 80 °C higher that in the unconfined solid.

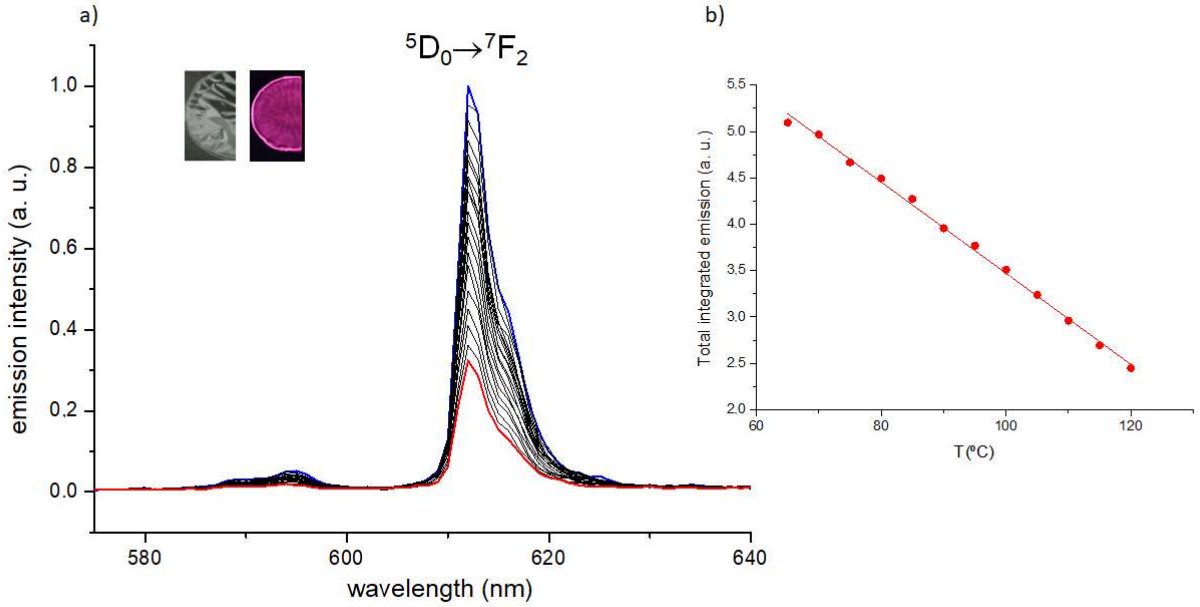

Fig. 10. (a) Normalized emission spectra of **1-PSU** relative to the most intense $^5D_0 \rightarrow {}^7F_2$ transition band at 25 ºC, in the range 25 - 110 °C with a 5 °C step between each measurement ($\lambda_{exc.}$ = 315 nm). Inset images are **1-PSU** under daylight and 365nm UV light. (b) Linear fit found between 65 °C until 120 °C (y= -0.049x + 8.38, r^2 of 0.997 for the 12 points

3. Conclusion

The main novelty of the here presented new optical molecular thermometer is the ratiometric emission using transitions to two crystal-field sublevels of the same electronic level of $^5D_0 \rightarrow {}^7F_2$ transition.

This ratiometric method is based on the changes of the intensity and shape of the hypersensitive electric dipole transition band $^5D_0 \rightarrow {}^7F_2$, which is highly sensitive to the coordination environment around Eu^{3+} and can be rationalized by the two intensity ratios; I_{613}/I_{616} and I_{616}/I_{613} as a function of temperature.

Changes in the luminescence intensity, induced by temperature variation, are generally caused by the thermal activation of luminescence quenching mechanisms and consequent increases in the non-radiative

decay processes. For the compound presented here we also need to take into consideration the contribution of asymmetry induced by temperature increase. The final band intensities are then a balance between quenching phenomena and compound structure around Eu^{3+} centre, both affected by temperature in different ways.

Under different thermal conditions, S_r (% C^{-1}) was found to be in the range 0.45–7.0% C^{-1}, with regular increments from 20 to 100 ºC, with reproducible results within the acceptable used conditions.

Confinement of the complex in a polysulfone matrix induces rigidity in the structure, due to steric hindrance, preventing the unusual thermochromic behaviour recently discovered for the $[Eu(FOD)_4]$ anion. The presented ratiometric method is particularly interesting for measuring temperatures higher than 60 °C, where determination with other Eu^{3+} complexes usually fails due to the gradual decrease of luminescence intensities until residual values. Additionally, using this methodology, a new increasing parameter, I_{613}/I_{616} ratio, can be related and rationalized with increasing temperature.

The versatility of the $[Eu(FOD)_4]^-$ anion in terms of thermochromism enables the modulation of the emissive Eu^{3+} based species by simple cationic exchange, to which we believe will allow a considerable increment in the maximum temperature sensitization.

4. Experimental

General

Reagent grade chemicals were obtained from Aldrich and used without further purification.

Microanalyses for C and H were carried using a Thermo Finnigan-CE Instruments Flash EA 1112 CHNS series. FT-IR spectra (range 4000-400 cm^{-1}) were collected as KBr pellets (Sigma-Aldrich, FT-IR grade) using a Thermo Scientific Nicolet iS50 FT-IR spectrometer, by averaging 64 scans at a maximum resolution of 4 cm^{-1}. Analysis of the heated sample was performed by heating previously **1** in an oven and then prepare the KBr pellet, assuring that the pallet had a purple color during acquisition of the FT-IR spectra.

TGA curves were obtained using a Thermal Analysis Ta Q500-2207, with a scanning rate of 10 °C min^{-1}, with samples weighing around 8 mg in Aluminum crucibles. The calibration of the TGA equipment was made following the recommendation described in the manufacturer's manual.

Luminescence spectra were measured using a SPEX Fluorolog-3 Model FL3-22 spectrofluorimeter, with 1 nm slits and measurement step of 0.1 nm. Excitation wavelength was variable and between 344 and 354 nm. Lifetime measurements were run on a LKS.60 ns laser photolysis spectrometer from Applied Photophysics, with a Brilliant Q-Switch Nd:YAG laser from Quantel, using the second harmonic (λ_{exc} =344 nm (cool sample) and 355 nm (previously heated sample), laser pulse half-width equal to 6 ns) and luminescence quantum efficiencies were measured by the absolute method with an Integrated Sphere. All spectra are corrected with correction functions provided by the supplier following standard procedures. The luminescence decays were performed with a LS45-Perkin-Elmer spectrofluorometer using a time-drive mode with a pulsed xenon lamp. Repeatability was confirmed through 3 measurements.

Emission decays were obtained with spectral resolution of 2 nm, with a perpendicular geometry in relation with the laser excitation, by averaging between 2 to 10 measurements at each emission wavelength depending on the emission intensity of the sample. Luminescence decay traces at each wavelength were analyzed using least-squares fittings of the experimental data, using Solver from Microsoft Excel. Monitorization of luminescence with increasing temperature was performed using an optical fiber focusing a small amount of **1** while heating over a thermostatized heating plate (Argolab). Temperature range was from 25 to 110 °C. The experimental setup used for the experiments is presented in the supplementary material (Figure S1).

The mass spectra were acquired on a LCQ Fleet ion trap mass spectrometer equipped with an ESI ion source (Thermo Scientific TM) operated in the ESI positive and negative ion modes, using the with the following optimized parameters: ion spray voltage, ±4. 5 kV; capillary voltage, 16/-18 V; tube lens offset, -70/58 V; sheath gas (N_2), 40 arbitrary units; auxiliary gas (N_2), 20 arbitrary units; capillary temperature, 300 ºC. Spectra typically correspond to the average of 20–35 scans and were

recorded in the range between 70-1500 Da. Data acquisition and data processing were done with Thermo Xcalibur 2.3 software.

Synthetic procedures

Synthesis of [CHOL][Eu(FOD)$_4$] (1): 1 equivalent of NaFOD (0.0767 g, 0.241mmol) was added to a solution of EuFOD$_3$ (0.250 g, 0.241 mmol) previously dissolved in methanol. The reaction mixture was left stirring for 2 hours at room temperature. 1 equivalent of CHOLCl (0.034 g, 0.241 mmol) previously dissolved in a minimum of CH_2Cl_2 was added dropwise to the solution with constant stirring. The mixture was left under magnetic stirring for one hour. The solvent was removed under low pressure and the crude solid was dissolved in CH_2Cl_2. NaCl was removed by filtration and the neat white power was recovered after solvent evaporation with yield of 80%. Anal. Calcd. for $[C_5H_{14}NO][Eu(C_{10}H_{10}O_2F_7)_4]$: C, 36.67; H, 3.70%. Experimental; C, 36.61; H, 3,98. 1H-NMR δ(ppm): 5.51(s, H_α FOD), 4.03 (m, -CH_2 CHOL), 3.52 (m, -CH_2 CHOL), 3.26 (s, -CH_3 CHOL), 0.7 (s, -CH_3 FOD).

Synthesis of [CHOL][Eu(FOD)$_4$]-polysulfone (1-PSU): Polysulfone (0.0586 g) and [CHOL][Eu(FOD)$_4$] (0.0012 g) were left stirring in a closed vial with 5 mL CH_2Cl_2 until complete dissolution of the polysulfone. The resulting solution was then put in a loosely closed petri dish, and left evaporating overnight in a room with a controlled temperature of 21 °C. **1-PSU** membrane was collected from the petri dish and used without any further treatment.

Declaration of Competing Interest

The authors declare no conflicts of competing interest.

Acknowledgements

This work was supported by the Associated Laboratory for Sustainable Chemistry-Clean Processes and Technologies- LAQV which is financed by national funds from FCT/MEC (UID/QUI/50006/2019) and co-financed by the ERDF under the PT2020 Partnership Agreement (POCI-01-0145-FEDER – 007265) The NMR spectrometers are part of The National NMR Facility, supported by Fundação para a Ciência e a Tecnologia (RECI/BBB-BQB/0230/2012). We also thank to RNEM – Portuguese Mass Spectrometry Network, ref. LISBOA-01-0145-FEDER-022125, supported by FCT and Lisboa Regional Operational Programme (Lisboa2020). This work has been supported by Fundação para a Ciência e a Tecnologia through the contract nº IST-ID/077/2018 (Bernardo Monteiro), SFRH/BD/120985/2016 (Mani Outis). Cláudia C. L. Pereira thanks to Fundação para a Ciência e a Tecnologia, MCTES, for the Norma transitória DL 57/2016 Program Contract.

Keywords

lanthanides; luminescence; molecular thermometers; sensors; thermochromic behavior

References

[1] C. D. S. Brites, S. Balabhadra, L. D. Carlos, *Adv. Optical Mater*. **2018**, 1801239-1801269.

[2] J. Rocha, C. D. S. Brites, L. D. Carlos, *Chem. Eur. J.* **2016**, *22*, 14782 – 14795.

[3] S. M. Bruno, D. Ananias, F. A. A. Paz, M. Pillinger, A. A. Valente, L. D. Carlos, I. S. Gonçalves, *Dalton Trans.* **2015**, *44*, 488–492.

[4] J. Rocha, C. D. S. Brites, L. D. Carlos, *Chem. Eur. J.* **2016**, *22*, 14782–14795.

[5] R. D. L. Gaspar, P. R. Fortes, I. O. Mazali, F. A. Sigoli, I. M. Raimundo Jr., *ChemistrySelect* **2018**, *3*, 10491– 10501.

[6] D. V. Lapaev, V. G. Nikiforov, V. S. Lobkov, A. A. Knyazev, Y. G. Galyametdinov, *Optical Materials* **2018**, *75*, 787-795.

[7] D. Mara, F. Artizzu, B. Laforce, L. Vincze, K. Van Hecke, R. Van Deuna, A. M. Kaczmarek, *J. Lumin.* **2019**, *213*, 343–355.

[8] A. Abdallah, S. Freslon, X. Fan, A. Rojo, C. Daiguebonne, Y. Suffren, K. Bernot, G. Calvez, T. Roisnel, O. Guillou, *Inorg. Chem.* **2019**, *58*, 462−475.

[9] H. Kobayashi, M. Ogawa, R. Alford, P.L. Choyke, Y. Urano, *Chem. Rev.* **2010**, *110*, 2620–2640.

[10] D. Jaque, B. del Rosal, E. M. Rodríguez, L. M. Maestro, P. H. González, J. G. Solé, *Nanomedicine* **2014**, *9*, 1047–1062.

[11] X. Rao, T. Song, Junkuo, G. Yuanjing, C. Yu, Y. C. Wu, B. Chen, G. Qian, *J. Am. Chem. Soc*. **2013**, *135*, 15559−15564.

[12] S. K. Sharma, T. Kohler, J. Beyer, M. Fuchs, R. Gloaguen, J. Heitmann, *Phys. Chem. Chem. Phys.* **2019**, *21*, 16329-16336.

[13] M. Suzuki, V. Tseeb, K. Oyama, S. Ishiwata, *Biophys. J.* **2007**, *92*, L46-L48.

[14] L. R. Dacanin, M. D. Dramicanin, S. R. Lukic-Petrovic, D. M. Petrovic, M. G. Nikolic, *Radiat. Meas*. **2013**, *56*, 143–146.

[15] M. G. Nikolic, A. Z. Al-Juboori, V. Dordevic, M. D. Dramicanin, *Phys. Scr.* **2013**, *T157*, 014056.

[16] K. W. Meert, V.A. Morozov, A. M. Abakumov, J. Hadermann, D. Poelman and P. F. Smet, *Opt. Express* **2014**, *22*, A961

[17] Z. Liang, F. Qin, Y. Zheng, Z. Zhang, W. Cao, *Sens. Actuators A* **2016**, *238*, 215–219.

[18] V. Lojpur, S. Cúlubrk, M. Medicand M. Dramicanin, *J. Lumin.* **2016**, *170*, 467–471.

[19] A. Ciric, S. Stojadinovic, M. D. Dramicanin, *Opt. Mater.* **2018**, *85*, 261–266.

[20] J. Yuasa, R. Mukai, Y. Hasegawa, T. Kawai, *Chem. Commun.* **2014**, *50*, 7937-7940.

[21] B. Monteiro, M. Outis, H. Cruz, J. P. Leal, C. A. T. Laia, C. C. L. Pereira, *Chem. Commun*. **2017**, *53*, 850-853.

[22] J. Yuasa, R. Mukai, Y. Hasegawa, T. Kawai, *Chem. Commun*. **2014**, *50*, 7937-7940.

[23] A S. Souza, L. A. O. Nunes, I. G. N. Silva, F. A. M. Oliveira, L. L. da Luz, H. F. Brito, M. C. F. C. Felinto, Rute A. S. Ferreira, S. A. Júnior, L. D. Carlos, O. L. Malta, *Nanoscale* **2016**, *8*, 5327–5333.

[24] D. Jaque, F. Vetrone, *Nanoscale* **2012**, *4*, 4301–4326.

[25] L. Zhou, Q. Pang, F. Gong, J. Sun, W. Wanga, *Luminescence* **2009**, *24*, 363–366.

[26] R. D. Adati, J. H. S. K. Monteiro, L.P. Cardoso, D. H. de Oliveira, M. Jafelicci Jr., M. R. Davolos, *J. Braz. Chem. Soc., J. Braz. Chem. Soc*. **2019**, *30*, 1707-1716.

[27] V. Divya, R. O. Freire, M. L. P. Reddy, *Dalton Trans.* **2011**, *40*, 3257– 3268.

[28] K. Binnemans, in: Handbook on the Physics and Chemistry of Rare Earths (Eds.: K.A. Gschneidner, Jr., J.-C.G. Bünzli and V.K. Pecharsky), Elsevier, Amsterdam, 2005, Chapter 225.

[29] C. Du, B. Zhao, X-B. Chen, N. Birbilis, H. Yang, *Scientific Reports* **2016**, 29225-29239.

[30] C. D. S. Brites, P. P. Lima, N. J. O. Silva, A. Millán, V. S. Amaral, F. Palacio, L. D. Carlos, *Nanos-cale* **2012**, *4*, 4799–4829.

[31] Z. P. Wang, D. Ananias, A. C.-Sánchez, C. D. S. Brites, I. Imaz, D. Maspoch, J. Rocha, L. D. Carlos, *Adv. Funct. Mater.* **2015**, *25*, 2824−2830.

[32] S. F. Collins, G. W. Baxter, S. A. Wade, T. Sun, K. T. V. Grattan, Z. Y. Zhang, A. W. Palmer, *J. Appl. Phys.* **1998**, *84*, 4649-4654.

[33] R. Lisiecki, W. Ryba-Romanowski, *J. Alloys Comp.* **2020**, *814*, 152304-152313.

[34] J. Zhou, R. Lei, H. Wang, Y. Hua, D. Li, Q. Yang, D.Deng, Shiqing Xu, *Nanophotonics* **2019**, 2347–2358.

[35] X. Yang, Hua Zou, X. Sun, T. Sun, C. Guo, Y. Fu, C.-M. L. Wu, X. Qiao, F. Wang, *Adv. Optical Mater*. **2019**, 190033-190039.

[36] C. Mi, J. Zhou, F. Wang, G. Lin, D. Jin, *Chem. Mater.* **2019**, *31*, 9480−9487.

[37] F. V. Bussche, A. M. Kaczmarek, J. Schmidt, C. V. Stevens, P. Van Der Voort, *J. Mat. Chem. C* **2019**, *7*, 10972-10980.

[38] D. A. Gálico, I. O. Mazali, F. A. Sigoli, *J. Lumin.* **2017**, *192*, 224-230.

[39] H. Peng, M. I. Stich, J. Yu, L. N. Sun, L. H. Fischer, O. S. Wolfbeis, *Adv. Mater.* **2010**, *22*, 716–719.

[40] K. Jin, John M. Torkelson, *Macromolecules* **2016**, *49*, 14, 5092-5103.